Artificial Collinear Lagrangian Point Maintenance with Electric Solar Wind Sail

Lorenzo Niccolai, Andrea Caruso, Alessandro A. Quarta, and Giovanni Mengali

***Abstract*—This paper discusses the maintenance of an L_1-type artificial equilibrium point in the Sun-[Earth+Moon] circular restricted three-body problem by means of an Electric Solar Wind Sail. The reference configuration instability is compensated for with a feedback control law that adjusts the grid voltage as a function of the distance from the natural L_1 point. Two different control strategies are analyzed assuming the solar wind fluctuations to be modelled through a statistical approach.**

***Index Terms*—Electric Solar Wind Sail, artificial Lagrangian equilibrium point, solar wind fluctuations, circular restricted three-body problem**

I. Introduction

An Electric Solar Wind Sail (E-sail) is an innovative propulsion system, invented in 2004 by Pekka Janhunen [1], which generates a propulsive acceleration by exploiting the solar wind dynamic pressure through the electrostatic interaction between a grid of charged tethers and the solar wind ions. After an on-ground experimental campaign [2], [3], the first in-flight testing of E-sail technology is being attempted in a geocentric environment by flying a variant of the E-sail working principle, the plasma brake [4], [5], [6]. The latter is a deorbiting system, consisting of a single charged tether that interacts with ions in the ionosphere to generate a drag. The first test was tried by the Estonian satellite EstCube [7], but a failure to the tether unreel mechanism occurred [8]. Currently, the Finnish Aalto-1 [9] satellite is equipped with a plasma brake tether that should enable an end-of-life deorbiting [10].

The major advantage of an E-sail-based spacecraft over more conventional systems is in its capability of providing thrust without consuming any propellant mass [11], [12], [13], [14], in a similar way to a solar sail [15]. The latter however uses the interaction of the solar radiation pressure with a large and highly reflective surface. The peculiarity of propellantless propulsive systems allows exotic mission scenarios to be envisaged, such as the creation and maintenance of an artificial equilibrium point (AEP) in which the relative position of the spacecraft is constant with respect to the Sun and the [Earth+Moon]. Indeed, because an AEP requires a continuous propulsive acceleration to be used, such a mission application is especially well suited for both solar sails [16], [17] and E-sails [18], [19]. The equilibrium condition for an AEP maintenance may be obtained by considering either the Sun's gravity alone [20], [21] or, more accurately, by taking into account the Sun-[Earth+Moon] gravitational field, as is done in the circular [22] and in the elliptic [23] three-body problem. In particular, this paper studies an L_1-type AEP, generated by means of a continuous outward radial propulsive acceleration, capable of displacing the collinear Lagrangian point L_1 toward the Sun. The practical importance of such an AEP is because a spacecraft placed at this point could guarantee an early warning in case of catastrophic solar events [17], a critical information for on-Earth communications and for orbiting satellites, especially in view of future manned mission toward the Moon or Mars [24]. Other possible mission scenarios aimed at Solar System exploration and involving an AEP-based orbit have been proposed in the literature [25], [26], [27], [28].

The design of an L_1-type AEP mission is complicated by the fact that the dynamics of a spacecraft placed at such an equilibrium point is known to be intrinsically unstable, so that the maintenance of its equilibrium position can only be achieved by means of an active control system. As far as solar sails are concerned, the possibility of properly adjusting their thrust magnitude by means of electrochromic materials has been firstly proposed in Ref. [29]. This concept has been tested in space by the Japanese IKAROS mission [30], and applied to AEP-maintenance in Refs. [16], [17]. In principle, a solar balloon can also be used as a sort of spherical solar sail, instead of a conventional flat (or nearly flat) reflective surface. When the balloon is inflated with gas, it expands (contracts) as the solar distance decreases (increases), with the effect of adjusting the propulsive acceleration magnitude and passively maintaining the spacecraft in the vicinity of the collinear AEP [31]. However, preliminary results obtained with typical values of the thermo-mechanical properties of the film material coating the solar balloon are not promising, and suggest that the contribution of such a passive control system to orbital stability is negligible [32]. As far as an E-sail propulsion system is considered, the only way to guarantee an L_1-type AEP maintenance is by means of an active control system that modifies the E-sail grid voltage as a function of the spacecraft heliocentric position and velocity.

The aim of this paper is to preliminarily investigate the

Manuscript submitted XX September 2019. This work is supported by the University of Pisa, Progetti di Ricerca di Ateneo (Grant no. PRA-2018-44).

L. Niccolai, A. Caruso, A. A. Quarta, and G. Mengali are with the Department of Civil and Industrial Engineering, University of Pisa, Via G. Caruso 8, I-56122, Pisa, Italy (e-mails: lorenzo.niccolai@ing.unipi.it, andrea.caruso@ing.unipi.it, a.quarta@ing.unipi.it, g.mengali@ing.unipi.it).

two-dimensional dynamics of an E-sail-based spacecraft near an L_1-type AEP in the presence of an active control system capable of modulating the grid electric voltage, in order to estimate the performance level necessary for orbital maintenance. The analysis is first conducted under the assumption of constant solar wind properties. Then, in analogy with the recent approach of Refs. [33], [34], the variability of the solar environment is taken into account by modelling the solar wind dynamic pressure as a random variable, of which the statistical distribution is reconstructed from available *in-situ* measurements. In this latter case, the control law design is much more involved, since the electric voltage modulation also depends on the solar wind dynamic pressure fluctuations. The analysis discussed in this work is confined to collinear L_1-type AEPs and assumes an early solar warning mission scenario, in which AEPs lie on the Ecliptic plane and are located between the Sun and the [Earth+Moon]. Indeed, an AEP placed above or below the Ecliptic plane would be more demanding to obtain in terms of required propulsive acceleration magnitude, without any advantage in terms of early warning time compared to an AEP placed on the Ecliptic. Moreover, unlike an out-of-plane AEP, the maintenance of a collinear L_1-type Lagrangian point requires a stable Sun-facing configuration [35], in which the spacecraft main body (including the communication subsystem) is located along the Sun-Earth line. On the other hand, ground communications could be interfered by the Sun's activity if the spacecraft were located exactly on the L_1-type AEPs. In fact, in that case, the telemetry signal would be mixed in the (strong) background solar radiation, which would lead to a too low value of the signal-to-noise ratio. For this reason, a scientific mission towards an L_1-type AEPs should plan the use of a (large enough) artificial Lissajous orbit. Finally, note that the transfer phase, from launch to the design AEP, is not considered this analysis. In fact, since an E-sail is capable of providing thrust only when there is no shielding action due to a planetary magnetic field, the velocity increment required to leave the Earth's magnetosphere must be provided by the upper stage of the launch vehicle, while the heliocentric transfer phase has been investigated elsewhere [36] in an optimal framework.

The manuscript is structured as follows. First, paralleling the procedure proposed by Aliasi et al. [22], a mathematical model describing the spacecraft dynamics around an L_1-type AEP is given, using the recent E-sail thrust model [37] to describe the propulsive acceleration magnitude and its direction. Then, an active control system is introduced in the model, and its capability of generating a stable dynamics around the AEP is investigated. The results are first presented by considering a deterministic space environment, and then by considering the fluctuations of the solar wind dynamic pressure. In the latter case the control law is suitably modified. Finally, the conclusion section summarizes the main outcomes on the work, and suggests possible future developments.

II. Mathematical model

Consider a spacecraft with a continuous-thrust propulsion system, which is moving within the Sun-[Earth+Moon] gravitational field. The spacecraft total mass m is negligible when compared to the Sun's mass $m_\odot$ and the [Earth+Moon]'s mass $m_\oplus$, so that the celestial bodies cover a circular orbit around their barycenter, without being affected by the presence of the spacecraft. It is convenient to use the standard notation of the circular restricted three-body problem (CR3BP). To that end, introduce a three-dimensional Cartesian synodic reference frame $\mathcal{T}(C; \hat{\boldsymbol{i}}, \hat{\boldsymbol{j}}, \hat{\boldsymbol{k}})$ with unit vectors $\{\hat{\boldsymbol{i}}, \hat{\boldsymbol{j}}, \hat{\boldsymbol{k}}\}$, of which the origin C is located at the system's barycenter. The unit vector $\hat{\boldsymbol{i}}$ lies along the Sun-Earth line, $\hat{\boldsymbol{k}}$ is perpendicular to the Ecliptic, and $\hat{\boldsymbol{j}}$ completes the right-handed frame; see Fig. 1. Finally, the spacecraft and the propulsive acceleration vector always lie on the Ecliptic.

Let G denote the universal gravitational constant, $\mu \triangleq m_\oplus/(m_\oplus + m_\odot) \approx 3.0404 \times 10^{-6}$ the dimensionless mass of [Earth+Moon], and $l \triangleq 1\,\text{au}$ the Sun-[Earth+Moon] reference distance. Note that l is constant in the CR3BP and is used as a scaling length of the problem. Accordingly, the Sun and the [Earth+Moon] are placed at a distance $l\,\mu$ and $l\,(1-\mu)$ from C, respectively. The dimensionless position vectors of the spacecraft with respect to the Sun, the [Earth+Moon], and the system's barycenter C, are referred to as $\boldsymbol{\rho}_\odot$, $\boldsymbol{\rho}_\oplus$, $\boldsymbol{r}$, respectively, with $\rho_\odot \triangleq \|\boldsymbol{\rho}_\odot\|$ and $\rho_\oplus \triangleq \|\boldsymbol{\rho}_\oplus\|$; see Fig. 1. With simple geometrical considerations, these vectors are related to each other by the following expressions

$$\boldsymbol{\rho}_\oplus = \boldsymbol{\rho}_\odot - \hat{\boldsymbol{i}} \quad , \quad \boldsymbol{r} = \boldsymbol{\rho}_\odot - \mu\,\hat{\boldsymbol{i}} \tag{1}$$

Let $\omega_\oplus\,\hat{\boldsymbol{k}}$ be the constant angular velocity of the synodic reference frame $\mathcal{T}$ with respect to an inertial reference frame, where $\omega_\oplus \triangleq \sqrt{G\,(m_\odot + m_\oplus)/l^3} = 2\,\pi\,\text{rad/year}$. The scaling time of the CR3BP is chosen to be $\omega_\oplus^{-1} = \sqrt{l^3/G\,(m_\odot + m_\oplus)}$. In analogy with Refs. [22], [38], the spacecraft equation of motion in the CR3BP may be written in dimensionless terms as

$$\ddot{\boldsymbol{r}} + 2\,\hat{\boldsymbol{k}} \times \dot{\boldsymbol{r}} + \hat{\boldsymbol{k}} \times \left(\hat{\boldsymbol{k}} \times \boldsymbol{r}\right) + \frac{1-\mu}{\rho_\odot^3}\,\boldsymbol{\rho}_\odot + \frac{\mu}{\rho_\oplus^3}\,\boldsymbol{\rho}_\oplus = \boldsymbol{a} \tag{2}$$

where $\boldsymbol{a}$ is the dimensionless propulsive acceleration vector. In Eq. (2), the dot symbol denotes a derivative taken with respect to the dimensionless time $\omega_\oplus\,t$, which may equivalently be converted into a derivative with respect to a polar angle (measured counterclockwise from a generic inertially-fixed direction) by recalling that $\omega_\oplus$ is constant.

A. L_1-type AEP

Equation (2) can be specialized to describe the orbital dynamics of a spacecraft placed at an L_1-type AEP. In that case, illustrated in Fig. 2, the spacecraft is at an equilibrium position in the synodic reference frame $\mathcal{T}$, and lies on the Sun-Earth line at a (dimensionless) distance $\rho_{\odot_0} \in (0,\,1)$ from the Sun, viz.

$$\boldsymbol{\rho}_{\odot_0} = \rho_{\odot_0}\,\hat{\boldsymbol{i}} \tag{3}$$

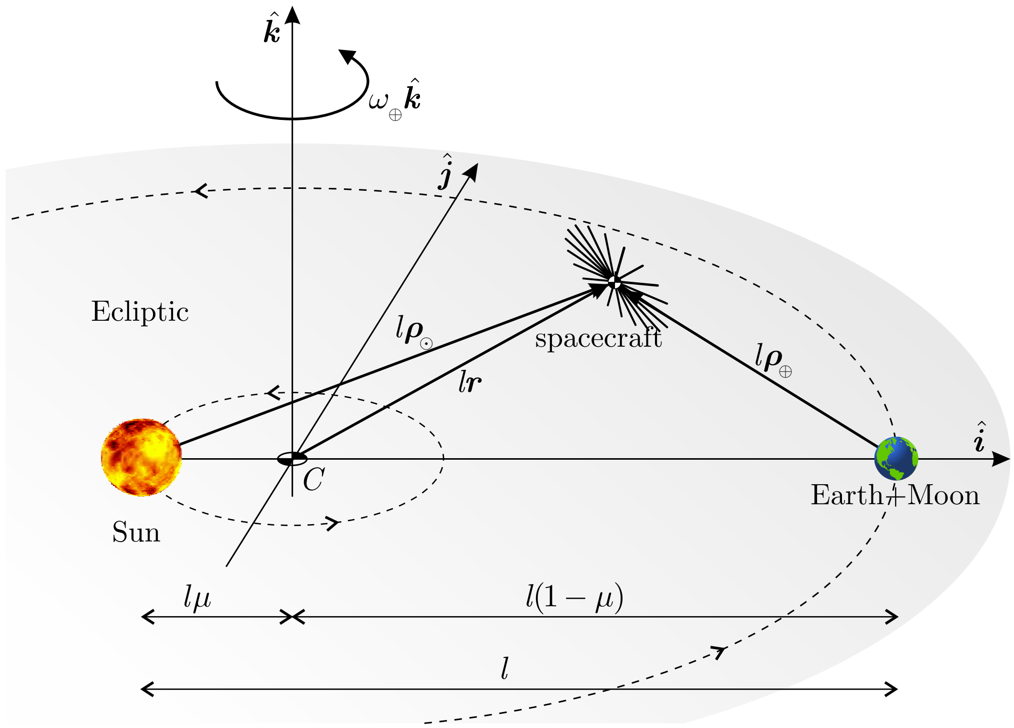

Figure 1. Geometrical sketch of the planar circular restricted three-body problem (CR3BP). Adapted from Ref. [22].

where the subscript 0 identifies a nominal and unperturbed condition.

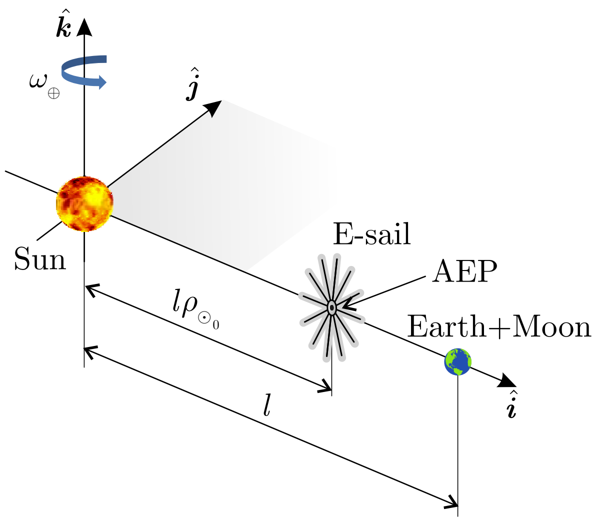

Figure 2. Sketch of the AEP maintenance mission scenario. Adapted from Ref. [33].

From Eqs. (1), the position vector $\boldsymbol{r}_0$ and the Earth-spacecraft vector $\boldsymbol{\rho}_{\oplus_0}$ can be rewritten as

$$\boldsymbol{\rho}_{\oplus_0} = -\left(1-\rho_{\odot_0}\right)\hat{\boldsymbol{\imath}} \qquad , \qquad \boldsymbol{r}_0 = \left(\rho_{\odot_0}-\mu\right)\hat{\boldsymbol{\imath}} \tag{4}$$

To maintain such an AEP, the time derivatives of the position and velocity vectors must be set equal to zero, that is

$$\ddot{\boldsymbol{r}}_0 = \dot{\boldsymbol{r}}_0 = 0 \tag{5}$$

When Eqs. (3)–(5) are substituted into Eq. (2), the latter provides the equilibrium condition along the radial direction, or

$$\boldsymbol{a}_0 = \left[-\left(\rho_{\odot_0}-\mu\right) + \frac{1-\mu}{\rho_{\odot_0}^2} - \frac{\mu}{\left(1-\rho_{\odot_0}\right)^2}\right]\hat{\boldsymbol{\imath}} \tag{6}$$

which gives the required dimensionless propulsive acceleration $\boldsymbol{a}_0$ for an L_1-type AEP maintenance. Note that the direction of $\boldsymbol{a}_0$ must be along the Sun-spacecraft line. Equation (6) is general, in that it is independent of the specific propulsion system, and must therefore be specialized to the E-sail case by introducing a suitable thrust model.

B. E-sail thrust model

The recent E-sail thrust model proposed by Huo et al. [37] is here used to describe the spacecraft propulsive acceleration vector $\boldsymbol{a}$. Starting from the results of Ref. [39], Huo et al. express the thrust vector $\boldsymbol{T}$ generated by an E-sail as

$$\boldsymbol{T} = m\,\tau\,\frac{a_c}{2}\left(\frac{1}{\rho_\odot}\right)\left[\hat{\boldsymbol{\rho}}_\odot + \left(\hat{\boldsymbol{\rho}}_\odot\cdot\hat{\boldsymbol{n}}\right)\hat{\boldsymbol{n}}\right] \tag{7}$$

where $\hat{\boldsymbol{\rho}}_\odot \triangleq \boldsymbol{\rho}_\odot/\rho_\odot$ is the Sun-spacecraft unit vector, $\hat{\boldsymbol{n}}$ is the unit vector normal to the E-sail nominal plane in the direction opposite to the Sun, $\tau \in \{0, 1\}$ is a dimensionless parameter that models the possibility of switching either on ($\tau \equiv 1$) or off ($\tau \equiv 0$) the electron gun that maintains the E-sail grid voltage, and a_c denotes the characteristic acceleration, that is, the maximum magnitude of the propulsive acceleration at a Sun-spacecraft distance equal to l. According to Ref. [37], the characteristic acceleration is

$$a_c = \frac{0.18\, N\, L}{m}\,(V - V_\mathrm{w})\,\sqrt{\epsilon_0\, p_\oplus} \simeq \frac{0.18\, N\, L\, V}{m}\,\sqrt{\epsilon_0\, p_\oplus} \tag{8}$$

where N is the number of tethers of the grid, L is the tether length, V is the grid voltage, V_w is the electric potential corresponding to the kinetic energy of the solar wind ions, ϵ_0 is the vacuum permittivity, and $p_\oplus$ is the solar wind dynamic pressure at 1 au from the Sun. The approximated final expression of Eq. (8) is justified by the fact that V is on the order of tens of kV [40], whereas V_w is about 1 kV only [37]. The value of a_c depends on the E-sail design parameters, the grid voltage and the environmental conditions. As such, as long as the fluctuations of the solar wind dynamic pressure are neglected and the grid voltage is fixed, a_c is constant.

Because an L_1-type AEP can be maintained by means of a continuous thrust only, the switching parameter is $\tau \equiv 1$; see Eq. (8). Moreover, the required propulsive acceleration is purely radial, see Eq. (6), and so the E-sail is always at a Sun-facing condition (that is, $\hat{\boldsymbol{n}} \equiv \hat{\boldsymbol{\rho}}_\odot$), even when the spacecraft position does not perfectly match that of the AEP. Note that the assumption of a Sun-facing E-sail attitude is supported by the recent results of Refs. [35], [41], [42], which state that the Sun-facing attitude is a stable configuration for a spinning and axially-symmetric E-sail with a uniform grid voltage. In this case, bearing in mind Eq. (7) and the definition of $\{l,\, \omega_\oplus\}$, the dimensionless propulsive acceleration vector is given by

$$\boldsymbol{a} = \frac{a_c\, l^2}{G\,(m_\oplus + m_\odot)}\left(\frac{1}{\rho_\odot}\right)\hat{\boldsymbol{\rho}}_\odot \tag{9}$$

In analogy with Ref. [22], Eq. (9) can be conveniently rewritten as

$$\boldsymbol{a} = \frac{\beta\,(1-\mu)}{\rho_\odot}\,\hat{\boldsymbol{\rho}}_\odot \tag{10}$$

where β is a dimensionless performance parameter, defined as

$$\beta \triangleq \frac{a_c}{G\, m_\odot / l^2} \tag{11}$$

Note that β is proportional to the characteristic acceleration, and its value coincides with the ratio of the maximum propulsive acceleration that the E-sail can generate at a distance of 1 au from the Sun to the local gravity attraction.

Substituting Eq. (10) into Eq. (6), the nominal value of lightness number necessary for maintaining an L_1-type AEP is

$$\beta_0 = \beta_{0_{L_1}} \triangleq \frac{1}{\rho_{\odot_0}} - \frac{\mu\,\rho_{\odot_0}}{1-\mu}\left[\frac{\rho_{\odot_0}}{\mu} - 1 + \frac{1}{(1-\rho_{\odot_0})^2}\right] \tag{12}$$

The corresponding characteristic acceleration a_{c_0} required for orbital maintenance is obtained from the definition of β (see Eq. (11)), since $a_{c_0} = \beta_{0_{L_1}}\,(G\, m_\odot / l^2) \simeq 5.93\, \beta_{0_{L_1}}\ \mathrm{mm/s^2}$.

III. Linear stability of an L_1-type AEP

The stability of an L_1-type AEP can be investigated with a linear approach. Paralleling the discussion of Ref. [31] for a solar sail-based spacecraft, the state vector of the dynamical system and its derivative are defined as

$$\boldsymbol{x} \triangleq \begin{bmatrix} x - \rho_{\odot_0} + \mu \\ y \\ \dot{x} \\ \dot{y} \end{bmatrix} \quad , \quad \dot{\boldsymbol{x}} \triangleq \begin{bmatrix} \dot{x} \\ \dot{y} \\ \ddot{x} \\ \ddot{y} \end{bmatrix} \tag{13}$$

where x and y (or $\dot{x}$ and $\dot{y}$) are the components of the position (or velocity) vector, which are measured in the synodic reference frame $\mathcal{T}$ along the radial ($\hat{\boldsymbol{\imath}}$) and the transverse ($\hat{\boldsymbol{\jmath}}$) direction, respectively. The state vector $\boldsymbol{x}$ is decomposed into the sum of the nominal (equilibrium) state $\boldsymbol{x}_0$, corresponding to the AEP, and a small perturbation vector $\delta\boldsymbol{x} = [\delta x,\, \delta y,\, \delta\dot{x},\, \delta\dot{y}]^\mathrm{T}$ such that

$$\boldsymbol{x} = \boldsymbol{x}_0 + \delta\boldsymbol{x} \equiv \delta\boldsymbol{x} \tag{14}$$

Note that out-of-plane perturbations (both in position and velocity components) are not included in this analysis. In fact, it is well known that they would generate an oscillating dynamics along the $\hat{\boldsymbol{k}}$-direction, without affecting the system stability.

Substituting Eq. (14) into Eq. (2), subtracting the unperturbed solution expressed by Eq. (6), and neglecting the second-order perturbation terms, the dynamics of the linearized system can be written in matrix form as

$$\dot{\boldsymbol{x}} = \mathbb{A}\,\boldsymbol{x} \tag{15}$$

where

$$\mathbb{A} \triangleq \begin{bmatrix} 0 & 0 & 1 & 0 \\ 0 & 0 & 0 & 1 \\ a_{31} & 0 & 0 & 2 \\ 0 & a_{42} & -2 & 0 \end{bmatrix} \tag{16}$$

with

$$a_{31} = 2 + \frac{2\,\mu}{(1-\rho_{\odot_0})^3} + \frac{1-\mu}{\rho_{\odot_0}^3} - \frac{\mu}{\rho_{\odot_0}} + \frac{\mu}{\rho_{\odot_0}\,(1-\rho_{\odot_0})^2} \tag{17}$$

$$a_{42} = \frac{\mu}{\rho_{\odot_0}} - \frac{\mu}{\rho_{\odot_0}\,(1-\rho_{\odot_0})^3} \tag{18}$$

For a given value of $\rho_{\odot_0} \in (0,\, 1)$, the matrix $\mathbb{A}$ has one eigenvalue with positive real part, and so the two-dimensional dynamics of an E-sail-based spacecraft in the vicinity of an L_1-type AEP is intrinsically unstable, in accordance with the results of Refs. [22], [31]. A suitable control system is therefore required to maintain the artificial collinear point.

A. Active control system

The previous analysis has shown that the maintenance of an L_1-type AEP is possible only by means of an active control system, of which the aim is to adjust the E-sail grid voltage V in order to modify the characteristic acceleration value a_c (or β); see Eqs. (8) or (11). The performance parameter is therefore written as $\beta = \beta_0 + \delta\beta$, where β_0

is given by Eq. (12) and $\delta\beta$ is the contribution due to the grid voltage variation, which is assumed to be sufficiently small. The linearized equation of the system becomes

$$\dot{\boldsymbol{x}} = \mathbb{A}\,\boldsymbol{x} + \mathbb{B}\,\delta\beta \tag{19}$$

where $\mathbb{A}$ is given by Eq. (16), and $\mathbb{B}$ is defined as

$$\mathbb{B} \triangleq \begin{bmatrix} 0 \\ 0 \\ (1-\mu)/\rho_{\odot_0} \\ 0 \end{bmatrix} \tag{20}$$

A proportional-derivative feedback control law is now introduced, in the form

$$\delta\beta = -\mathbb{K}\,\boldsymbol{x} \tag{21}$$

with

$$\mathbb{K} \triangleq \begin{bmatrix} k_1 & 0 & k_2 & 0 \end{bmatrix} \tag{22}$$

where $k_1 \geq 0$ is the proportional gain, whereas $k_2 \geq 0$ is the derivative gain, that is, $\delta\beta = -k_1\,\delta x - k_2\,\delta\dot{x}$. The dynamics of the controlled system becomes

$$\dot{\boldsymbol{x}} = (\mathbb{A} - \mathbb{B}\,\mathbb{K})\;\boldsymbol{x} = \mathbb{C}\,\boldsymbol{x} \tag{23}$$

and the system stability depends on the eigenvalues of the matrix $\mathbb{C} \triangleq \mathbb{A} - \mathbb{B}\,\mathbb{K}$, where $\mathbb{A}$, $\mathbb{B}$, and $\mathbb{K}$ are given by Eqs. (16), (20), and (22), respectively. Recalling the definitions of matrices $\{\mathbb{A}, \mathbb{B}, \mathbb{K}\}$, the stability of an L_1-type AEP only depends on μ (which is determined by Sun's and [Earth+Moon]'s masses), on the nominal Sun-spacecraft distance $\rho_{\odot_0}$, and on the control gains $\{k_1, k_2\}$.

B. Case of fluctuating solar wind dynamic pressure

The thrust model used so far and expressed by Eqs. (7)–(8) is based on the assumption that the solar wind dynamic pressure $p_\oplus$ is time-constant and isotropic (i.e., it is independent of heliocentric latitude and polar angle). While isotropy is fairly realistic in a two-dimensional dynamics, the time invariance is not supported by *in-situ* measurements, which instead reveals that the solar wind is highly unpredictable and the dynamic pressure has a chaotic behaviour [43]. Indeed, the fluctuations of the solar wind dynamic pressure are on the same order of magnitude as its mean value and show almost no regularity. To verify the effectiveness of the proposed control laws in a realistic environment, the value of $p_\oplus$ in Eq. (8) is therefore conservatively modelled as a random variable, of which the instantaneous value is independent of the previous ones, in accordance with the approach of Refs. [33], [34]. The probability density function (PDF) used to model $p_\oplus$ is artificially-reconstructed, based on available experimental measurements, with the procedure discussed in Ref. [34].

A grid voltage adjustment in response to a fluctuating solar wind dynamic pressure $p_\oplus$ is assumed in analogy with Refs. [33], [34], [44], [45], and is obtained as follows. First, the total flight time T is divided into legs of 1 day. Previous studies suggest that the length of time legs does not significantly affect the results, as soon as the selected value is on the order of some hours [34]. At the beginning of each leg, a value of $p_\oplus$ is randomly generated, with the PDF given in Ref. [34], and the E-sail grid voltage is adjusted so as to meet the nominal value of the performance parameter β_0. In practice, recalling that $V_\mathrm{w} \ll V$, the desired grid voltage V_opt at the beginning of a (generic) leg, is found as

$$V_\mathrm{opt}(t) = V_0 \sqrt{\frac{\overline{p}_\oplus}{p_\oplus(t)}} \tag{24}$$

where $\overline{p}_\oplus \triangleq 2\,\mathrm{nPa}$ is the mean value of the solar wind dynamic pressure at 1 au from the Sun, and $V_0 \triangleq 25\,\mathrm{kV}$ is the nominal E-sail grid voltage [40]. However, because the E-sail grid voltage cannot exceed a maximum value, a saturation constraint on V is introduced, that is,

$$V \leq V_\mathrm{max} \tag{25}$$

where V_max is the maximum allowable value of V. The voltage adjustment is therefore

$$V(t) = \begin{cases} V_\mathrm{opt}(t) & \text{if} \quad V_\mathrm{opt}(t) \leq V_\mathrm{max} \\ V_\mathrm{max} & \text{if} \quad V_\mathrm{opt}(t) > V_\mathrm{max} \end{cases} \tag{26}$$

where V_opt is given by Eq. (24). Note that, unlike Refs. [34], [33], no constraint is introduced on the maximum allowable voltage variation. Indeed, preliminary results suggest that the typical characteristic time required for grid voltage adjustment is on the order of a few minutes only. The new value of $\beta_0(t)$ is obtained by combining Eqs. (8), (11) and (24), that is

$$\beta_0(t) = \begin{cases} \beta_{0_{L_1}} & \text{if} \quad V_\mathrm{opt}(t) \leq V_\mathrm{max} \\ \beta_{0_{L_1}} \dfrac{V_\mathrm{max}}{V_0} \sqrt{\dfrac{p_\oplus(t)}{\overline{p}_\oplus}} & \text{if} \quad V_\mathrm{opt}(t) > V_\mathrm{max} \end{cases} \tag{27}$$

where $\beta_{0_{L_1}}$ and $V_\mathrm{opt}(t)$ are given by Eqs. (12) and (24), respectively. Then, $p_\oplus$ (and so β_0) is kept constant throughout the leg, and Eq. (2) is integrated with an orbital propagator until the end of the leg, when a new value of $p_\oplus$ is generated and the procedure is restarted. The algorithm stops when the total desired flight time is reached, that is, $t \equiv T$.

IV. Numerical simulations

As discussed in the previous section, the stability of an L_1-type AEP in the Sun-[Earth+Moon] gravitational field only depends on $\rho_{\odot_0}$ and the control gains $\{k_1, k_2\}$. However, the necessary performance level of the E-sail is also influenced by the value of $\rho_{\odot_0}$, so that an AEP close to the Sun could be theoretically stable, but practically impossible to be maintained due to the severe technology requirements. Three possible values of Sun-AEP distance $l\,\rho_{\odot_0}$ have been considered, that is, $l\,\rho_{\odot_0} = [0.987730,\, 0.980521,\, 0.943555]\,\mathrm{au}$, corresponding to $a_{c_0} = [0.1,\, 0.3,\, 1]\,\mathrm{mm/s^2}$, which are compatible with a near-, mid- or far-term technology level, respectively. In a solar warning mission case [17], the selected values of Sun-AEP distance could guarantee an early warning time of about

[1.27, 2.02, 5.86] hours, with a substantial improvement compared to that of NASA's ACE mission [46], which is tracking a Lissajous orbit around L_1 since 1997, with a warning time of about 1 hour.

To check the stability of the controlled system, the eigenvalues of the $\mathbb{C}$ matrix are calculated for each value of $\rho_{\odot_0}$ as a function of the control gains $\{k_1, k_2\}$; see Eq. (23). Then, some numerical tests are performed by simulating the orbital dynamics of an E-sail by means of a variable order Adams-Bashforth-Moulton solver scheme [47], [48]. The initial conditions are chosen in the vicinity on an L_1-type AEP, with a small initial perturbation $\delta\boldsymbol{x}_{\text{in}} \triangleq \delta\boldsymbol{x}(t_{\text{in}})$ (with $t_{\text{in}} \triangleq 0$) which models an orbital insertion error. According to Folta et al. [49], the initial errors in the Earth-Moon gravitational field may be set equal to 1 km (position error) and 1 cm/s (velocity error) in each direction. In our case, taking into account the different length and time scales of the Earth-Moon CR3BP with respect to the Sun-[Earth+Moon] CR3BP, the position (or velocity) error is increased by three (or two) order of magnitudes, thus obtaining an initial position error of 1000 km and an initial velocity error of 1 m/s in both radial and transverse directions. These values, when expressed in dimensionless form in the synodical frame $\mathcal{T}$, are

$$\delta\boldsymbol{x}_{\text{in}} = \begin{bmatrix} 6.684 \times 10^{-6} \\ 6.684 \times 10^{-6} \\ 3.357 \times 10^{-5} \\ 3.357 \times 10^{-5} \end{bmatrix} \tag{28}$$

The vector $\delta\boldsymbol{x}_{\text{in}}$ of Eq. (28) is used as the initial perturbation for all simulations. Two cases will now be discussed, according to whether the solar wind dynamic pressure is constant or modeled as a random variable.

A. *Proportional control law*

Assume first that the grid voltage is adjusted with a simple proportional feedback control. This amounts to setting $k_2 = 0$ in the $\mathbb{K}$ matrix of Eq. (22), so that the variation of β only depends on the radial distance from the spacecraft and the AEP, that is, $\delta\beta = -k_1\,\delta x$.

Figure 3 shows the real parts of the eigenvalues λ_i (with $i = 1, \ldots, 4$) of the closed-loop matrix as a function of k_1, using three different values of the nominal characteristic acceleration. Clearly, one eigenvalue has a positive real part when $k_1 < k^\star$, thus implying system instability. When $k_1 > k^\star$, instead, the AEP is marginally stable, that is, the perturbed dynamics oscillates in the vicinity of the nominal position. The value of $k^\star$ depends on the nominal characteristic acceleration a_{c_0} or, equivalently, on the Sun-AEP distance $\rho_{\odot_0}$. It may be verified that $k^\star \simeq 6.272$, 3.816, or 3.043, when $a_{c_0} = 0.1$, 0.3, or 1 mm/s^2, respectively, as is illustrated in Fig. 3.

Figure 4 shows the evolution of the spacecraft position on the Ecliptic calculated with an orbital propagator, assuming $l\,\rho_{\odot_0} = 0.980521$ au (that is, $a_{c_0} = 0.3$ mm/s^2) and $k_1 = 5$, which corresponds to a marginally stable condition. Recall that the initial perturbation vector is

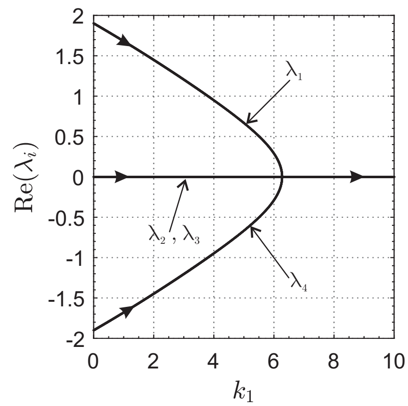

(a) $a_{c_0} = 0.1$ mm/s^2.

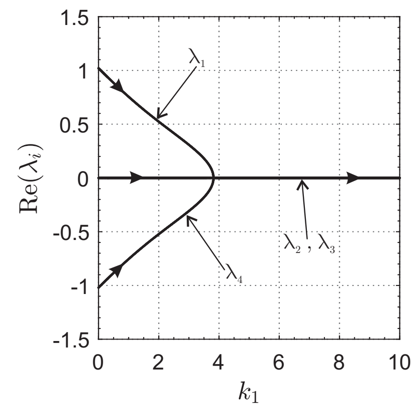

(b) $a_{c_0} = 0.3$ mm/s^2.

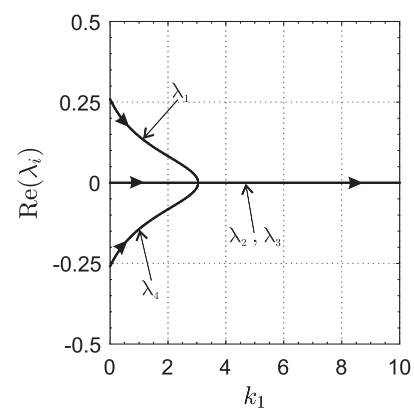

(c) $a_{c_0} = 1$ mm/s^2.

Figure 3. Real parts of eigenvalues λ_i ($i = 1, \ldots, 4$) as a function of k and a_{c_0} for a proportional control law.

given by Eq. (28), while the total simulated flight time is $T = 50$ years. The motion remains bounded in the vicinity of the AEP (marked with a green point) and the maximum distance from the AEP is 4.93×10^{-5} au $\simeq$ 7 381 km. The maximum variation of β with respect to its nominal value given by Eq. (12) is on the order of 0.35% only. In other terms, an orbital maintenance is possible with very small variations of the grid voltage only, since V is directly proportional to β; see Eqs. (8) and (11). The simulations obtained with other values of $\rho_{\odot_0}$ and k_1

provide similar results, and are not reported here for the sake of conciseness.

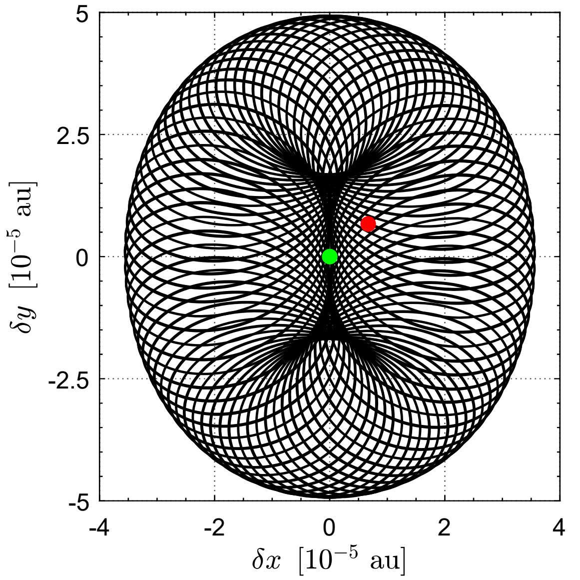

Figure 4. Two-dimensional distance with respect to the AEP (green point) for a E-sail-based spacecraft with proportional control system ($k_1 = 5$, $k_2 = 0$) with initial conditions given by Eq. (28) (red point).

B. Proportional-derivative control law

The previous discussion has shown that a purely-proportional feedback control system can only generate an oscillatory dynamics around the AEP. If the spacecraft is required to return in the vicinity of the nominal position, a proportional-derivative control law could solve the problem. In this case the gains k_1 and k_2 in the $\mathbb{K}$ matrix of Eq. (22) are both different from zero, and β becomes a function of the radial distance from the AEP and the radial component of the spacecraft velocity, that is, $\delta\beta = -k_1\delta x - k_2\delta\dot{x}$.

The real parts of the eigenvalues λ_i (with $i = 1, \ldots, 4$) of the closed-loop matrix are shown in Fig. 5 as a function of a_{c_0} and of the gains, which, in analogy with Ref. [31], are assumed to take the same numerical value, that is, $k_1 = k_2 = k$. Figure 5 shows that a stable dynamics is possible only if $k > k^\star$, where $k^\star$ coincides with the value found with a proportional control law. This result confirms that the stability of the system is influenced by the proportional gain k_1 only, whereas the derivative gain k_2 introduces some damping in the motion along the radial component. Indeed, a proportional-derivative control law (with $k > k^\star$) guarantees all of the eigenvalues to have negative real part, which implies an asymptotically stable motion around the L_1-type AEP. However, because the real part of the dominant pole has a very small modulus, the system approaches the design AEP with a slow dynamics.

Figure 6 shows the two-dimensional dynamics of the system starting in the vicinity of an AEP with $l\,\rho_{\odot_0} =$

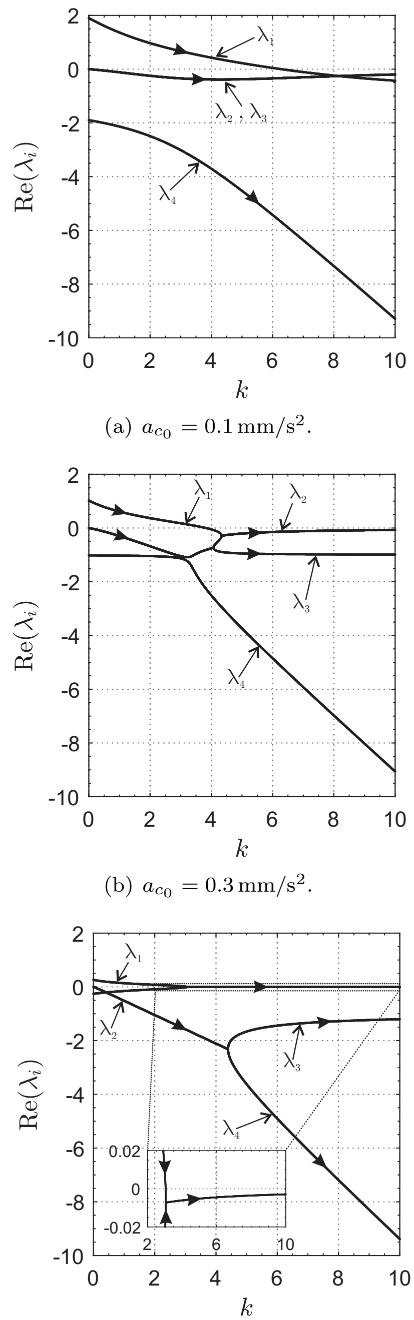

(a) $a_{c_0} = 0.1\,\mathrm{mm/s^2}$.

(b) $a_{c_0} = 0.3\,\mathrm{mm/s^2}$.

(c) $a_{c_0} = 1\,\mathrm{mm/s^2}$.

Figure 5. Real parts of eigenvalues λ_i ($i = 1, \ldots, 4$) as a function of k and a_{c_0} for a proportional-derivative control law.

$0.980521\,\mathrm{au}$ (corresponding to $a_{c_0} = 0.3\,\mathrm{mm/s^2}$). The proportional and derivative gains are chosen as $k_1 = k_2 = 5$, and the total simulated flight time is $T = 50\,\mathrm{years}$. In this case, the maximum distance between the AEP and the E-sail is $3.02 \times 10^{-5}\,\mathrm{au} \simeq 4\,514\,\mathrm{km}$, whereas the maximum required variation of grid voltage amounts to 0.40% of the nominal value. These values both have the same order of magnitude than those found in the proportional control case. Even though the derivative gain gives an asymptotical convergence to the AEP, the settling time is long, since the spacecraft-AEP distance is still larger than 1000 km after 1 year and becomes practically negligible only after 4 years of flight time. Therefore, the advantages with respect to a proportional control system are not substantial from a mission design viewpoint.

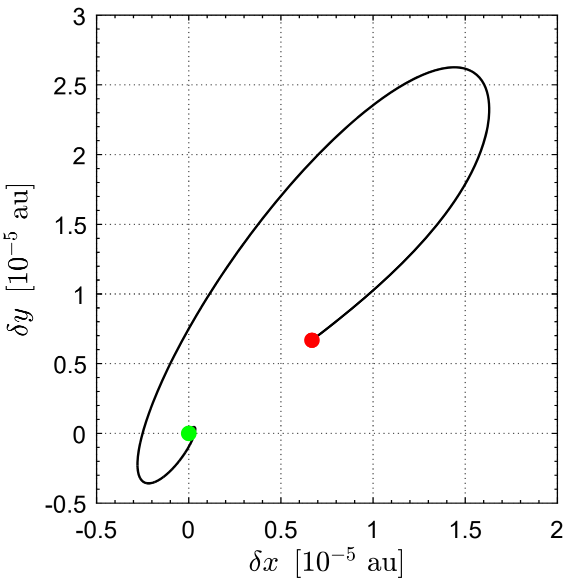

Figure 6. Two-dimensional distance with respect to the AEP (green dot) for a E-sail-based spacecraft with proportional-derivative control system ($k_1 = k_2 = 5$) and initial conditions given by Eq. (28) (red dot).

Other simulations have been performed by further increasing the derivative gain k_2, but the results do not substantially change, while the voltage variations imposed by the control system increase up to unfeasible values. These considerations suggest that a proportional-derivative control system does not guarantee a sufficient improvement with respect to a proportional control, since the characteristic time required to damp out the oscillations around the AEP are long, when compared to a typical mission duration of an orbiting spacecraft. Therefore, taking into account the increased complexity of the control system, and the difficulty of accurately measuring the radial component of velocity (which is necessary in a proportional-derivative control), a simple proportional control probably represents the best compromise solution between performance and complexity.

Finally, the proposed control law has also been tested in a more complex scenario, that is, in an elliptic restricted framework, in which the actual eccentricity of the [Earth+Moon] heliocentric orbit is taken into account. The mathematical model used in the numerical simulations has been adapted from Ref. [16]. The numerical results are obtained by simulating a total flight time $T = 50$ years with the same initial conditions and control gains used for the simulations reported in Figs. 4 and 6. Using a proportional control law the maximum AEP-spacecraft distance is 7.23×10^{-4} au $\simeq$ 108 184 km, while using a proportional-derivative control law this value reduces to 4.04×10^{-4} au $\simeq$ 60 010 km, with a settling time further increased with respect to the circular case. The maximum lightness number variation amounts to 3.06% (or 1.30%) of the nominal value for the proportional (or proportional-derivative) control law case, including the contribution required to compensate the Sun-AEP distance variation due to planetary orbital eccentricity. These results show that the [Earth+Moon]'s orbital eccentricity does not change the control law effectiveness, and that the (pulsating) AEP maintenance is still feasible and compatible with typical mission requirements. The previous considerations about the CR3BP case, according to which a proportional control system is a good compromise between performance and complexity, still apply to the elliptic case.

C. Results with a varying solar wind dynamic pressure

The performance of a proportional control system in a CR3BP framework are now verified in a more realistic environment, in which the solar wind dynamic pressure is time-varying. Using the above described procedure, a numerical simulation with $l\,\rho_{\odot_0} = 0.980521$ au and $\delta \boldsymbol{x}_{\text{in}}$ of Eq. (28) is performed for a total flight time of $T = 10$ years, comparable with the duration of a deep space mission. Because the results of Refs. [33], [34] suggest a large saturation voltage to be required for orbital maintenance, a value of $V_{\max} = 80$ kV is chosen for the simulations. A number of 100 simulations have been performed, and the mean value of the distance is about 26 123 km, while the global maximum amounts to 176 335 km. For exemplary purposes, Fig. 7 shows a time-history of the radial coordinate, which compares the AEP position (green line) with the perturbed trajectories in the synodic frame, obtained by assuming either a constant (black line) or a variable (blue line) solar wind dynamic pressure. Although the distance from the AEP has increased with respect to the previous cases, the spacecraft is still able to provide an early warning in case of catastrophic solar events. Finally, note that the introduction of an out-of-plane perturbation (both in position and velocity) does not significantly affect the results even in presence of a fluctuating solar wind dynamic pressure. Indeed, the mean and maximum values of the position error are very close to that obtained for the planar case.

V. Conclusions

A spacecraft propelled by an Electric Solar Wind Sail may generate an artificial equilibrium point in the Sun-[Earth+Moon] gravitational field. In particular, with reference to an L_1-type artificial equilibrium point, its orbital maintenance is complicated by the intrinsic instability of such a position. However, a control system capable of adjusting the grid voltage of the Electric Solar Wind Sail is able to overcome this issue.

A proportional and a proportional-derivative control law have been discussed with a linear approach, which allows the minimum values of the system gains necessary for stability to be obtained numerically. The voltage variations imposed by the control system and the

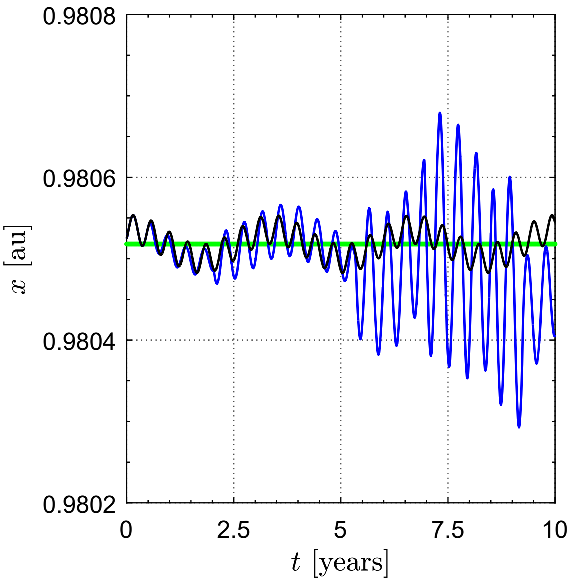

Figure 7. Time history of the radial coordinate x with $\rho_{\odot 0} = 0.980521$ in the case of constant (black) or fluctuating (blue) solar wind dynamic pressure with $V_{\max} = 80\,\mathrm{kV}$, compared with the AEP position (green).

maximum distances from the nominal position are found to be small. A proportional control system could only guarantee marginal stability (with an oscillating dynamics), while a proportional-derivative control system may provide asymptotic stability. However, since in the latter case the characteristic times are on the order of years, the former solution is advisable, due to its design simplicity. The proportional control system may be effectively used even when the random fluctuations of the solar wind dynamic pressure are taken into account. Further work will concentrate on the inclusion of the orbital eccentricity of the primary bodies, and on the control problem within a three-dimensional dynamics. In particular, the impact of electromagnetic interferences generated by grid charging and discharging on the communication subsystem needs to be better analyzed and quantified. In this regard, a possible research extension is about the development of a control law for applications to Lissajous orbits around the (design) artificial equilibrium point.

Acknowledgments

This work is supported by the University of Pisa, Progetti di Ricerca di Ateneo (Grant no. PRA-2018-44).

References

[1] P. Janhunen, "Electric sail for spacecraft propulsion," *Journal of Propulsion and Power*, vol. 20, no. 4, pp. 763–764, July-August 2004.

[2] P. Janhunen, P. K. Toivanen, J. Polkko, S. Merikallio, P. Salminen, E. Haeggstrom, H. Seppanen, R. Kurppa, J. Ukkonen, S. Kiprich, G. Thornell, H. Kratz, L. Richter, O. Kromer, R. Rosta, M. Noorma, J. Envall, S. Latt, G. Mengali, A. A. Quarta, H. Koivisto, O. Tarvainen, T. Kalvas, J. Kauppinen, A. Nuottajarvi, and A. Obraztsov, "Electric solar wind sail: Towards test missions," *Review of Scientific Instruments*, vol. 81, no. 11, pp. 111 301 (1–11), 2010.

[3] H. Seppänen, T. Rauhala, S. Kiprich, J. Ukkonen, M. Simonsson, R. Kurppa, P. Janhunen, and E. Haeggstrom, "One kilometer (1 km) electric solar wind sail tether produced automatically," *Review of Scientific Instruments*, vol. 84, no. 9, September 2013.

[4] P. Janhunen, "Electrostatic plasma brake for deorbiting a satellite," *Journal of Propulsion and Power*, vol. 26, no. 2, pp. 370–372, March–April 2010.

[5] ——, "Simulation study of the plasma-brake effect," *Annales Geophysicae*, vol. 32, pp. 1207–1216, 2014.

[6] L. Orsini, L. Niccolai, G. Mengali, and A. A. Quarta, "Plasma brake model for preliminary mission analysis," *Acta Astronautica*, vol. 144, pp. 297–304, March 2018.

[7] S. Latt, A. Slavinskis, E. Ilbis *et al.*, "Estcube-1 nanosatellite for electric solar wind sail in-orbit technology demonstration," *Proceedings of the Estonian Academy of Sciences*, vol. 63, no. 2S, pp. 200–209, 2014.

[8] A. Slavinskis, M. Pajusalu, H. Kuuste *et al.*, "Estcube-1 in-orbit experience and lessons learned," *IEEE Aerospace and Electronic Systems Magazine*, vol. 30, no. 8, pp. 12–22, August 2015.

[9] A. Kestila, T. Tikka, P. Peitso *et al.*, "Aalto-1 nanosatellite - technical description and mission objectives," *Geoscientific Instrumentation, Methods and Data Systems*, vol. 2, pp. 121–130, 2013.

[10] O. Khurshid, T. Tikka, J. Praks, and M. Hallikainen, "Accomodating the plasma brake experiment on-board the Aalto-1 satellite," *Proceedings of the Estonian Academy of Sciences*, vol. 63, no. 2S, pp. 258–266, 2014.

[11] A. Sanchez-Torres, "Propulsive force in an electric solar sail for outer planet missions," *IEEE Transactions on Plasma Science*, vol. 43, no. 9, Sep. 2015.

[12] ——, "Propulsive force in electric solar sail for missions in the heliosphere," *IEEE Transactions on Plasma Science*, vol. 47, no. 3, pp. 1657–1662, Mar. 2019.

[13] M. Huo, S. Cao, Y. Liu, H. Liao, and N. Qi, "Mission analyisis for Vesta and Ceres exploration using electric sail with classical and advanced thrust models," *IEEE Transactions on Aerospace and Electronic Systems*, 2019, in press.

[14] M. Huo, G. Zhang, N. Qi, Y. Liu, and X. Shi, "Initial trajectory design of electric solar wind sail based on finite fourier series shape-based method," *IEEE Transactions on Aerospace and Electronic Systems*, vol. 55, no. 6, pp. 3674–3683, 2019.

[15] C. R. McInnes, *Solar Sailing: Technology, Dynamics and Mission Applications*, ser. Springer-Praxis Series in Space Science and Technology. Berlin: Springer-Verlag, 1999, pp. 13–14, 46–54.

[16] G. Aliasi, G. Mengali, and A. A. Quarta, "Artificial Lagrange points for solar sail with electrochromic material panels," *Journal of Guidance, Control and Dynamics*, vol. 36, no. 5, pp. 1544–1550, September 2013.

[17] G. Vulpetti, C. Circi, and T. Pino, "Coronal mass ejection early-warning mission by solar-photon sailcraft," *Acta Astronautica*, vol. 140, pp. 113–125, November 2017.

[18] G. Mengali and A. A. Quarta, "Non-keplerian orbits for electric sails," *Celestial Mechanics and Dynamical Astronomy*, vol. 105, no. 1–3, pp. 179–195, November 2009.

[19] G. Aliasi, G. Mengali, and A. A. Quarta, "Artificial equilibrium points for electric sails with constant attitude," *Journal of Spacecraft and Rockets*, vol. 50, no. 6, pp. 1295–1298, November 2013.

[20] L. Niccolai, A. A. Quarta, and G. Mengali, "Electric sail elliptic displaced orbits with advanced thrust model," *Acta Astronautica*, vol. 138, pp. 503–511, September 2017.

[21] ——, "Electric sail-based displaced orbits with a refined thrust model," *Proceedings of the Institution of Mechanical Engineers. Part G, Journal of Aerospace Engineering*, vol. 232, no. 3, pp. 423–432, March 2018.

[22] G. Aliasi, G. Mengali, and A. A. Quarta, "Artificial equilibrium points for a generalized sail in the circular restricted three-body problem," *Celestial Mechanics and Dynamical Astronomy*, vol. 110, no. 4, pp. 343–368, August 2011.

[23] ——, "Artificial equilibrium points for a generalized sail in the elliptic restricted three-body problem," *Celestial Mechanics and Dynamical Astronomy*, vol. 114, no. 1-2, pp. 181–200, October 2012.

[24] N. F. Pissarenko, "Radiation environment due to galactic and solar cosmic rays during manned mission to Mars in the periods

between maximum and minimum solar activity cycles," *Advances in Space Research*, vol. 14, no. 10, pp. 771–778, October 1994.

[25] G. Mengali, A. A. Quarta, and P. Janhunen, "Considerations of electric sailcraft trajectory design," *JBIS-Journal of the British Interplanetary Society*, vol. 61, no. 8, pp. 326–329, August 2008.

[26] R. J. McKay, M. Macdonald, M. Vasile, and F. Bosquillon de Frescheville, "A novel interplanetary communications relay," in *AIAA/AAS Astrodynamics Specialist Conference*, Toronto (ON), Canada, 2–5 August 2010.

[27] C. Bombardelli, "Stable artificial equilibrium points in the Mars-Phobos system," in *1st IAA Conference on Dynamics and Control of Space Systems (DyCoss)*, Porto, Portugal, 19–21 March 2012.

[28] M. Zamaro and J. D. Biggs, "Identification of new orbits to enable future mission opportunities for the human exploration of the Martian moon Phobos," *Acta Astronautica*, vol. 119, pp. 160–182, February 2016.

[29] C. Jack and C. S. Welch, "Solar kites: Small solar sails with no moving parts," *Acta Astronautica*, vol. 40, no. 2–8, pp. 137–142, January–April 1997.

[30] R. Funase, O. Mori, Y. Tsuda, Y. Shirasawa, T. Saiki, Y. Mimasu, and J. Kawaguchi, "Attitude control of IKAROS solar sail spacecraft and its flight results," in *61st International Astronautical Congress*, Prague, Czech Republic, September–October 2010.

[31] J. D. Biggs and C. R. McInnes, "Passive orbit control for space-based geo-engineering," *Journal of Guidance, Control and Dynamics*, vol. 33, no. 3, pp. 1017–1020, May-June 2010.

[32] G. Aliasi, G. Mengali, and A. A. Quarta, "Passive control feasibility of collinear equilibrium points with solar balloons," *Journal of Guidance, Control, and Dynamics*, vol. 35, no. 5, pp. 1657–1661, September-October 2012.

[33] L. Niccolai, A. Anderlini, G. Mengali, and A. A. Quarta, "Impact of solar wind fluctuations on electric sail mission design," *Aerospace Science and Technology*, vol. 82–83, pp. 38–45, November 2018.

[34] ——, "Electric sail displaced orbit control with solar wind uncertainties," *Acta Astronautica*, vol. 162, pp. 563–573, Sep. 2019.

[35] M. Bassetto, G. Mengali, and A. A. Quarta, "Thrust and torque vector characteristics of axially-symmetric E-sail," *Acta Astronautica*, vol. 146, pp. 134–143, May 2018.

[36] A. A. Quarta, G. Aliasi, and G. Mengali, "Electric solar wind sail optimal transit in the circular restricted three body problem," *Acta Astronautica*, vol. 116, pp. 43–49, 2015.

[37] M. Huo, G. Mengali, and A. A. Quarta, "Electric sail thrust model from a geometrical perspective," *Journal of Guidance, Control, and Dynamics*, vol. 41, no. 3, pp. 734–740, 2018.

[38] R. H. Battin, *An Introduction to the Mathematics and Methods of Astrodynamics*. AIAA, 1987, ch. 8, pp. 371–381.

[39] P. K. Toivanen and P. Janhunen, "Thrust vector of an electric solar wind sail with a realistic sail shape," *Acta Astronautica*, vol. 131, pp. 145–151, February 2017.

[40] P. Janhunen, A. A. Quarta, and G. Mengali, "Electric solar wind sail mass budget model," *Geoscientific Instrumentation, Methods and Data Systems*, vol. 2, no. 1, pp. 85–95, 2013.

[41] M. Bassetto, G. Mengali, and A. A. Quarta, "Stability and control of spinning electric solar wind sail in heliostationary orbit," *Journal of Guidance, Control and Dynamics*, vol. 42, no. 2, pp. 425–431, 2019.

[42] ——, "Attitude dynamics of an electric sail model with a realistic shape," *Acta Astronautica*, vol. 159, pp. 250–257, 2019.

[43] N. Meyer-Vernet, *Basics of the Solar Wind*. Cambridge University Press, 2007, ch. 6, pp. 291–333.

[44] P. K. Toivanen and P. Janhunen, "Electric sailing under observed solar wind conditions," *Astrophysics and Space Sciences Transactions*, vol. 5, no. 1, pp. 61–69, 2009.

[45] ——, "Spin plane control and thrust vectoring of electric solar wind sail," *Journal of Propulsion and Power*, vol. 29, no. 1, pp. 178–185, Jan. 2013.

[46] E. C. Stone, A. M. Frandsen, R. A. Mewaldt, E. R. Christian, D. Margolies, J. F. Ormes, and F. Snow, "The Advanced Composition Explorer," *Space Science Reviews*, vol. 86, no. 1–4, pp. 1–22, 1998.

[47] L. F. Shampine and M. K. Gordon, *Computer Solution of Ordinary Differential Equations: The Initial Value Problem.* San Francisco: W. H. Freeman, 1975, ch. 10.

[48] L. F. Shampine and M. W. Reichelt, "The MATLAB ODE suite," *SIAM Journal on Scientific Computing*, vol. 18, no. 1, pp. 1–22, January 1997.

[49] D. C. Folta, T. A. Pavlak, K. C. Howell, M. A. Woodard, and D. W. Woodfork, "Stationkeeping of lissajous trajectories in the Earth-Moon system with applications to ARTEMIS," in *AAS/AIAA Space Flight Mechanics Meeting*, San Diego (CA), USA, February 2010, pp. 193–208.

Lorenzo Niccolai received his Ph.D. degree in Aerospace Engineering from the University of Pisa in 2018, and is currently a Research Assistant with the same institution. His research interests include mission design, low-thrust trajectory analysis and control, with special attention on innovative propulsive concepts such as solar sails and electric solar wind sails.

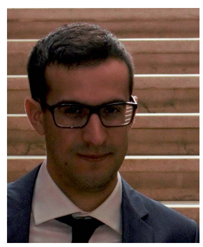

Andrea Caruso is a Ph.D. student in Aerospace Engineering from the University of Pisa, where he received his M.S. degree in 2016. His research activity is mainly focused in mission analysis and trajectory optimization for low-thrust propulsion systems, including solar sails and electric solar wind sails.

Alessandro A. Quarta received his Ph.D. degree in Aerospace Engineering from the University of Pisa in 2005, and is currently Professor of Flight Mechanics at the Department of Civil and Industrial Engineering of the University of Pisa. His main research areas include spaceflight simulation, spacecraft mission analysis and design, low-thrust trajectory optimization, solar sail and E-sail dynamics and control.

Giovanni Mengali received the Doctor Engineer degree in Aeronautical Engineering in 1989 from the University of Pisa. Since 1990 he has been with the Department of Aerospace Engineering (now Department of Civil and Industrial Engineering) of the University of Pisa, first as a Ph.D. student, then as an Assistant and an Associate Professor. Currently, he is Professor of Space Flight Mechanics. His main research areas include spacecraft mission analysis, trajectory optimization, solar sails, electric sails and aircraft flight dynamics and control.